

Novel Single-mode Narrow-band Photon Source of High Brightness for Hybrid Quantum Systems

Amir Moqanaki,¹ Francesco Massa,¹ and Philip Walther¹

¹*Faculty of Physics, University of Vienna, Boltzmannngasse 5, A-1090 Vienna, Austria*

(Dated: March 11, 2019)

Cavity-enhanced Spontaneous parametric down-conversion (SPDC) is capable of efficient generation of single photons with suitable spectral properties for interfacing with the atoms. However, beside the remarkable progress of this technique, multi-mode longitudinal emission remains as major drawback. Here we demonstrate a bright source of single photons that overcomes this limitation by a novel mode-selection technique based on the introduction of an additional birefringent element to the cavity. This enables us to tune the double resonance condition independent of the phase matching, and thus to achieve single-mode operation without mode filters. Our source emits single-frequency-mode photons at 852 nm, which is compatible to the Cs D2 line, with a bandwidth of 10.9 MHz and a photon-pair generation rate exceeding 47 KHz at 10 mW of pump power, while maintaining a low $g^{(2)}(0) = 0.13$. The efficiency of our source is further underlined by measuring a four-photon generation rate of 37 Hz at 20 mW of pump power. This brightness opens up a variety of new applications reaching from hybrid light-matter interactions to optical quantum information tasks based on long temporal coherence.

I. INTRODUCTION

Single photons' mobility, efficient detection, and ease of manipulation make them the system of choice for observing many quantum phenomena^{1,2} and the natural choice for quantum information processing applications³⁻⁷. However, the lack of photon-photon interactions raises the challenge to implement two-qubit gates⁸. One promising strategy to overcome this, is interfacing single photons with the strong optical non-linearities provided by matter-based quantum systems⁹⁻¹². Such hybrid quantum systems, with the combined benefits of both photons and matter, can realize quantum devices such as two-qubit gates, quantum memories, quantum repeaters, and eventually a full-scale quantum network¹³. Spontaneous parametric down-conversion (SPDC) has been widely used to generate high-purity single photons¹⁴ at broad range of frequencies at room temperature. In contrast to other photon generation techniques^{15,16}, SPDC also allows for efficient photon heralding. Recent developments in periodic poling and laser-written waveguides have triggered the realization of bright, robust and tunable photon sources^{17,18}.

The bandwidth of photons that are generated via SPDC is in the order of hundreds of GHz to THz¹⁹⁻²¹, which is orders of magnitude broader than the few MHz linewidth of typical atomic transitions. One obvious method for narrowing the bandwidth is passive spectral filtering. However, this leads to significant losses, making such techniques very inefficient²².

It has been shown that an optical parametric oscillator (OPO) pumped well below its threshold can emit single photons within the bandwidth of its cavity and greatly enhance the spectral brightness^{23,24}. Since the SPDC bandwidth is typically larger than the free-spectral range (FSR) of the enhancement cavity, the resulting source has

a multi-mode spectral characteristic²⁵⁻²⁸. Additional filters such as filter cavities^{25-27,29} and atomic line filters³⁰ have been employed to suppress these unwanted modes. But introducing these mode-filtering stages comes at the cost of photon loss and increased complexity of the setup. Recently, doubly resonant OPOs have opened up the possibility to use the so-called *cluster effect* and exploit its frequency-selectivity to enable narrow-band photon sources to perform with significantly fewer modes³¹⁻³⁴. Reaching the necessary doubly resonant condition for the cluster effect is unfortunately not trivial and has been mainly attempted at highly non-degenerate SPDC³²⁻³⁴, or has not been sufficient to directly generate single mode narrow-band photons yet³¹.

In this work we report a novel approach to reach doubly resonant condition by inserting an additional birefringent crystal in a type-II OPO and tuning the clustering independent of the SPDC phase-matching. In this way, we are able to obtain a single cluster within the SPDC bandwidth and reaching single-mode operation. Tuning the cluster effect allows us to generate photons at a broad range frequencies, covering the degenerate case. The measured number of generated longitudinal modes from our source is to our knowledge the lowest ever reported. Our mode-selection scheme minimizes photon losses because of the additional filtering, and enhancing the generation rate, which even allows us to directly observe more than one photon-pair emission from our source.

II. SINGLE-MODE OPERATION

In a doubly resonant OPO, SPDC emission can occur only in the signal and idler longitudinal modes that are both resonant to the cavity at the same time. Due to birefringence or frequency dependence of the refractive index of optical components, signal and idler modes can have different FSRs. In this case, not every signal mode

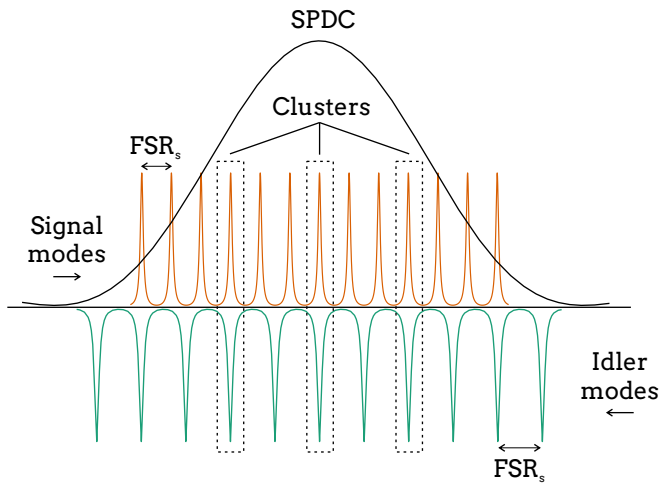


FIG. 1. **Cluster effect.** The longitudinal modes for signal are shown in orange, and the modes for idler are in green. The two arrows indicate the direction in which frequency increases. For maximum SPDC gain, both signal and idler should be resonant at the center of the SPDC bandwidth (black solid curve), as depicted in the figure. The overlap condition is periodical, but because of the difference in the FSRs for signal and idler, the modes that are next to the fully overlapping ones coincide only partially. This leads to a spectrum that is made of clusters of modes, separated by $\Delta\nu_C$. In each cluster a bright central mode is surrounded by weaker neighboring modes. In a high finesse cavity, the linewidth of signal and idler modes are narrow enough to make the partial overlap negligible.

within the SPDC bandwidth is simultaneously resonant with a corresponding idler mode, and the resulting OPO spectrum is made of *clusters* of few modes instead of a comb-like pattern (see Fig. 1). This effect is known as the *cluster effect*³⁵⁻³⁸.

The clusters are separated by a combined FSR that is larger than both signal and idler FSRs, given by the relation below³⁵, in which $FSR_{s,i}$ are the FSR for the signal and the idler modes, respectively:

$$\Delta\nu_c = \frac{FSR_s \cdot FSR_i}{|FSR_s - FSR_i|}. \quad (1)$$

However, reaching the doubly resonant condition at a desired wavelength is not trivial. Because tuning the cluster effect involves modifying the refractive indices of the SPDC crystal for signal and idler, consecutively affecting the SPDC phase-matching condition and complicating the process. When we add another degree of freedom dedicated for tuning the cluster separation - without affecting phase-matching - then we can simplify the tuning. Previous works have already partially investigated this by angle tuning of the SPDC crystal or applying voltage across the crystal^{31,36}. Yet these efforts have not been sufficient to fully suppress the unwanted longitudinal modes.

We consider having a linear cavity with length d , which contains an SPDC crystal with length L , a birefringent crystal - which we call *tuning crystal* -, with length L' ,

and some air gap ($L_{gap} = d - L - L'$). We take n_s, n_i as the group indices for signal and idler at the tuning crystal, and n'_s, n'_i as the group indices at the SPDC crystal. The tuning crystal should be mounted such that the birefringence of the SPDC crystal is partially compensated, meaning that $(n_s - n_i)(n'_s - n'_i) < 0$. The tuning crystal length, L' , should not be long enough to fully compensate for the birefringence of the cavity, because in this case all the signal and idler modes would completely overlap and the clustering would not occur.

By using Eq. 1, for the cluster separation in this arrangement we obtain:

$$\Delta\nu_c = \frac{c}{2|n_s L - n_i L + n'_s L' - n'_i L'|}. \quad (2)$$

The additional degrees of freedom of the tuning crystal allows us to achieve the cluster effect at the desired frequencies, independent of the phase-matching condition, and, at the same time, increase the cluster separation such that only one cluster falls within the SPDC bandwidth.

This happens when $\Delta\nu_c > \Delta\nu_{SPDC}$, where $\Delta\nu_{SPDC} \approx c/2|n_s L - n_i L|$ is the half-width-half-maximum of the SPDC gain profile³⁹. By using equation 2, this condition becomes:

$$\frac{1}{2} \frac{|n_s - n_i|}{|n'_s - n'_i|} \leq \frac{L'}{L} < \frac{|n_s - n_i|}{|n'_s - n'_i|}. \quad (3)$$

This leads to emission of a single cluster which can still contain more than one mode (See Fig. 1). When the bandwidth of the modes is narrow enough such that the partial overlap determining the neighboring modes is negligible, each cluster contains only one mode. If we define $\Delta\nu_s$ and $\Delta\nu_i$ the bandwidth of signal and idler modes, respectively, which we can write this condition as:

$$\frac{1}{2}\Delta\nu_s + \frac{1}{2}\Delta\nu_i < |FSR_i - FSR_s|. \quad (4)$$

Approximating the same finesse, F , for both signal and idler, we set a minimum threshold for the finesse:

$$F > \frac{1}{2} \frac{FSR_i + FSR_s}{|FSR_i - FSR_s|}. \quad (5)$$

III. EXPERIMENTAL REALIZATION

We show a schematic of the experimental realization of the source in Fig.2. The probe laser (Toptica DL Pro 852, 50 mW) is tuned to the Cs D2 line and acts as the frequency reference. In order to lock the pump laser (Toptica DL Pro 426, 30 mW) to the probe laser, we frequency-double the probe by a single-pass type-I PP-KTP crystal (30mm, Raicol Crystals) to 426 nm. We

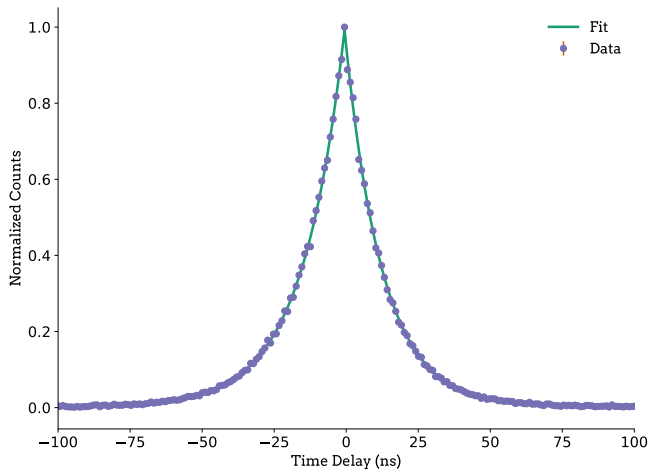


FIG. 3. **Experimental cross-correlation.** The delays are calculated from the coincidence time-tags recorded by the TTM. We normalize the counts to the maximum and correct for the accidentals and the dark counts. Each time bin has a width of 2.97 ns , which corresponds to six times the combined jitter of the detectors. The errorbars are calculated from the Poisson statistics of the photon counting. The fit function is an exponential (See Eq. 6) and the decay rates γ_s and γ_i are the fit parameters. The FWHM of the fit is $(18.7 \pm 0.5) \text{ ns}$, resulting into a bandwidth of $(10.9 \pm 0.3) \text{ MHz}$.

with a fit from Eq. 6. This cross-correlation signal is not symmetric, because of the birefringence in the OPO, which is not fully compensated by the tuning crystal. The cross-correlation time, calculated from the fit, is $(18.7 \pm 0.5) \text{ ns}$. Considering the doubly-resonant condition, the effective bandwidth of the photons is given by $\frac{0.64}{\pi\tau_c}$, which corresponds to a bandwidth of $(10.9 \pm 0.3) \text{ MHz}$ for the photon-pairs^{41,43}.

The auto-correlation function, $G^{(2)}(\tau)$ provides information about the statistics of the single SPDC fields. We measure this by splitting the signal arm with a 50:50 fiber beam splitter (Thorlabs TW850R5F1) and by recording the coincidences at the output ports at the time delay τ , thus realizing an Hanbury Brown-Twiss interferometer. Our results are plotted in Fig. 4.

Unlike the cross-correlation, $G^{(2)}(\tau)$ is symmetric and has a more complex shape (see Eq. 8). Ideally, the auto-correlation would peak at $G^{(2)}(0) = 2$ when being measured by a detection system with no time-jitter, thus revealing the thermal statistics of the SPDC fields. However, given the relatively large combined jitter in the detectors (0.495 ns) with respect to the correlation time (18.7 ns), this holds true only for a single-frequency-mode photon source, and in the multi-mode case the peak value decreases, $G^{(2)}(0) < 2$. In fact, the value of auto-correlation function at 0 delay gives the effective number of modes that are present in the cavity, N^{42} :

$$G^{(2)}(0) = 1 + \frac{1}{N} \quad (7)$$

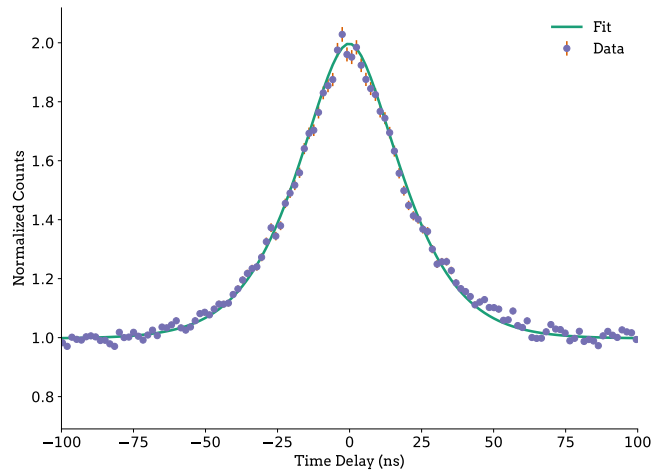


FIG. 4. **Experimental auto-correlation.** The delays are calculated from the coincidence time-tags recorded by the TTM. We normalize the counts to the value at far delays. The time bin size is 4.95 ns , which corresponds to ten times the combined jitter of our detectors. The errorbars are calculated from the Poisson statistics of the photon counting. The fit function is that of Eq. 8 and the fit parameters are γ_s and γ_i . The auto-correlation is symmetric and visibly broader than the cross-correlation. The auto-correlation time is calculated from the fit to be $41.1 \pm 0.5 \text{ ns}$, which is more than two times larger than the cross-correlation time, as expected. The peak value at 0 delay is 1.995 ± 0.001 , corresponding to single-frequency-mode operation.

The general expression for the auto-correlation when the signal and the idler experience different decay rates, $\gamma_s \neq \gamma_i$, is given by³³:

$$G^{(2)}(\tau) \approx 1 + \left[e^{-\frac{\gamma_s + \gamma_i}{2} |\tau|} \left(1 + \frac{\gamma_i + \gamma_s}{2} |\tau| \right) \right]^2. \quad (8)$$

By fitting the Eq. 8 to our experimental data, we obtain $G^{(2)}(0) = 1.995 \pm 0.001$. The errors are based on Poisson statistics and are obtained by Monte Carlo simulation of several runs⁴⁴. The auto-correlation function is expected to be broader than the cross-correlation function. We calculate the FWHM of the fit to be $41.1 \pm 0.5 \text{ ns}$, more than two times larger than τ_c as expected from the theoretical predictions. These results indicate that our source operates in a single-longitudinal mode^{33,42}.

Another parameter that is used for source characterization is the heralded or conditional second-order correlation function $g^{(2)}(\tau)$, which is measured in the same way as the auto-correlation, with the only difference that the detection of the signal photon is heralded by the corresponding detection of an idler photon. The value of this function at zero delay, $g^{(2)}(0)$ quantifies multiphoton emission from an SPDC source^{28,39}. This value should be $g^{(2)}(0) = 0$ for an ideal single-photon source without higher order emissions. We calculate $g^{(2)}(0)$ as³⁹:

$$g^{(2)}(0) = \frac{2 \times C_H \times CC_{\text{HAB}}}{(CC_{\text{HA}} + CC_{\text{HB}})^2}, \quad (9)$$

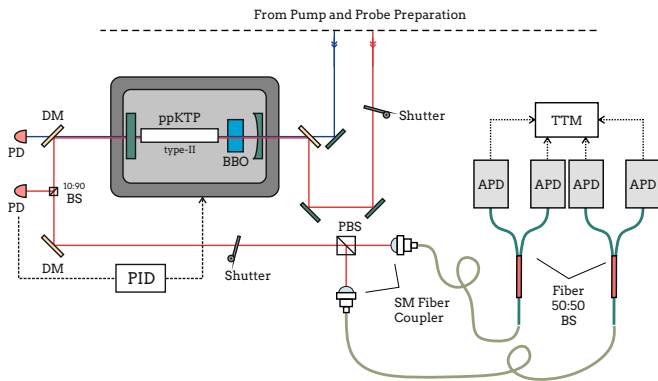


FIG. 5. **Set-up for the measurement of the 4-fold coincidences.** For the 4-fold coincidence measurement the pump power is increased and the double pairs are spatially separated by two 50:50 fiber beam-splitters. The 4-fold coincidences are post-selected by the TTM.

where C_H is the rate of single counts for the heralding photons, CC_{HA} , CC_{HB} are the 2-fold coincidence rates between the heralding photon and the two arms of the the Hanbury Brown-Twiss interferometer respectively, and CC_{HAB} is the 3-fold coincidence rate. We measure the heralded auto-correlation at 1 mW of pump power to be $g^{(2)}(0) = 0.04 \pm 0.01$, and at 10 mW of pump power to be $g^{(2)}(0) = 0.130 \pm 0.006$. The errors are calculated from the Poisson statistics on photon counting.

We record 2.5 KHz 2-fold coincidence counts at 10 mW of pump power. This corresponds to a photon-pair generation rate of 47.5 KHz after correcting for the coupling and detection loss, and the transmission of the dichroic filters, and thus to a spectral brightness of $436\text{ s}^{-1}\text{mW}^{-1}\text{MHz}^{-1}$. This single-mode photon-pair generation rate surpasses previous results based on bulk optics and additional mode filters at the same level of photon purity^{28,31,45,46}.

Our mode selection technique allows for direct single-mode emission, and therefore does not require any additional filtering stage. This drastically reduces the losses and gives us the possibility to operate the source at a new parameter regime such that multi-photon generation can be detected. In order to demonstrate this, we increase

the pump power to 20 mW and introduce an additional 50:50 BS (see Fig. 5) for being able to measure the 4-fold coincidences by probabilistically separating the photons into four output modes. At this pump power we measure a 4-fold coincidence rate of 0.28 Hz , and obtain a double-pair generation rate of 37 Hz after correcting for losses.

V. CONCLUSIONS

Here we experimentally demonstrate a novel technique to efficiently generate narrow-bandwidth single-frequency-mode photons. We characterize our source by analyzing the temporal correlations of the emitted photons. Furthermore, we show that our mode-selection approach reduces the losses to the level that makes multiphoton generation accessible to experimental investigation. Our work opens up the possibility to use narrow-band multi-photon states for applications such as verification of matter-based two-photon gates^{11,12}, multi-boson correlation sampling and richer temporal interference landscapes⁴⁷, and generation of highly entangled narrow-band states for quantum communication and quantum information processing⁴⁸.

ACKNOWLEDGMENTS

We would like to thank Kai-Hong Luo, Andreas Ahlrichs, Oliver Benson, and Morgan Mitchell for the useful discussions. We thank Fabian Laudenbach and the Austrian Institute of Technology (AIT) GmbH for kindly lending us their TTMs. We would like to thank European Commission under the project ErBeStA (No. 800942), Austrian Research Promotion Agency (FFG) through the QuantERA ERA-NET Cofund project HiPhoP, Austrian Science Fund (FWF) through the doctoral programme CoQuS (W1210), NaMuG (P30067-N36), and GRIPS (P30817-N36), University of Vienna via the Research Platform TURIS, and Red Bull GmbH for their generous support.

¹ M. Giustina, M. A. M. Versteegh, S. Wengerowsky, J. Handsteiner, A. Hochrainer, K. Phelan, F. Steinlechner, J. Kofler, J.-A. Larsson, C. Abellán, W. Amaya, V. Pruneri, M. W. Mitchell, J. Beyer, T. Gerrits, A. E. Lita, L. K. Shalm, S. W. Nam, T. Scheidl, R. Ursin, B. Wittmann, and A. Zeilinger, Phys. Rev. Lett. **115**, 250401 (2015).

² D. Bouwmeester, J.-W. Pan, K. Mattle, M. Eibl, H. Weinfurter, and A. Zeilinger, Nature **390**, 575 (1997).

³ A. Crespi, R. Osellame, R. Ramponi, D. J. Brod, E. F. Galvao, N. Spagnolo, C. Vitelli, E. Maiorino, P. Mataloni, and F. Sciarrino, Nature Photonics **7**, 545 (2013).

⁴ M. A. Broome, A. Fedrizzi, S. Rahimi-Keshari, J. Dove, S. Aaronson, T. C. Ralph, and A. G. White, Science **339**, 794 (2013).

⁵ J. B. Spring, B. J. Metcalf, P. C. Humphreys, W. S. Kolthammer, X.-M. Jin, M. Barbieri, A. Datta, N. Thomas-Peter, N. K. Langford, D. Kundy, J. C. Gates, B. J. Smith, P. G. R. Smith, and I. A. Walmsley, Science (2012).

⁶ M. Tillmann, B. Dakić, R. Heilmann, S. Nolte, A. Szameit, and P. Walther, Nature Photonics **7**, 540 (2013).

⁷ P. Walther, K. J. Resch, T. Rudolph, E. Schenck, H. Weinfurter, V. Vedral, M. Aspelmeyer, and A. Zeilinger, Nature

- 434**, 169 (2005).
- ⁸ E. Knill, R. Laflamme, and G. J. Milburn, *nature* **409**, 46 (2001).
 - ⁹ Q. A. Turchette, C. J. Hood, W. Lange, H. Mabuchi, and H. J. Kimble, *Physical Review Letters* **75**, 4710 (1995).
 - ¹⁰ H. Schmidt and A. Imamoglu, *Optics letters* **21**, 1936 (1996).
 - ¹¹ J. Volz, M. Scheucher, C. Junge, and A. Rauschenbeutel, *Nature Photonics* **8**, 965 (2014).
 - ¹² B. Hacker, S. Welte, G. Rempe, and S. Ritter, *Nature* **536**, 193 (2016).
 - ¹³ H. J. Kimble, *Nature* **453**, 1023 (2008).
 - ¹⁴ M. D. Eisaman, J. Fan, A. Migdall, and S. V. Polyakov, *Review of Scientific Instruments* **82**, 071101 (2011).
 - ¹⁵ P. Senellart, G. Solomon, and A. White, *Nature nanotechnology* **12**, 1026 (2017).
 - ¹⁶ B. Rodiek, M. Lopez, H. Hofer, G. Porrovecchio, M. Smid, X.-L. Chu, S. Gotzinger, V. Sandoghdar, S. Lindner, C. Becher, *et al.*, *Optica* **4**, 71 (2017).
 - ¹⁷ S. Tanzilli, H. De Riedmatten, W. Tittel, H. Zbinden, P. Baldi, M. De Micheli, D. B. Ostrowsky, and N. Gisin, *Electronics Letters* **37**, 26 (2001).
 - ¹⁸ M. Fiorentino, S. M. Spillane, R. G. Beausoleil, T. D. Roberts, P. Battle, and M. W. Munro, *Optics Express* **15**, 7479 (2007).
 - ¹⁹ B. E. Saleh, M. C. Teich, and B. E. Saleh, *Fundamentals of photonics* (Wiley New York, 2007).
 - ²⁰ M. H. Rubin, D. N. Klyshko, Y. Shih, and A. Sergienko, *Physical Review A* **50**, 5122 (1994).
 - ²¹ M. M. Fejer, G. Magel, D. H. Jundt, and R. L. Byer, *Quantum Electronics, IEEE Journal of* **28**, 2631 (1992).
 - ²² A. Haase, N. Piro, J. Eschner, and M. W. Mitchell, *Optics letters* **34**, 55 (2009).
 - ²³ Z. Y. Ou and Y. J. Lu, *Phys. Rev. Lett.* **83**, 2556 (1999).
 - ²⁴ Y. J. Lu and Z. Y. Ou, *Phys. Rev. A* **62**, 033804 (2000).
 - ²⁵ J. S. Neergaard-Nielsen, B. M. Nielsen, H. Takahashi, A. I. Vistnes, and E. S. Polzik, *Opt. Express* **15**, 7940 (2007).
 - ²⁶ M. Scholz, F. Wolfgramm, U. Herzog, and O. Benson, *Applied Physics Letters* **91**, 191104 (2007).
 - ²⁷ X.-H. Bao, Y. Qian, J. Yang, H. Zhang, Z.-B. Chen, T. Yang, and J.-W. Pan, *Phys. Rev. Lett.* **101**, 190501 (2008).
 - ²⁸ M. Rambach, A. Nikolova, T. J. Weinhold, and A. G. White, *APL Photonics* **2**, 119901 (2017).
 - ²⁹ A. Ahlrichs, C. Berkemeier, B. Sprenger, and O. Benson, *Applied Physics Letters* **103**, 241110 (2013).
 - ³⁰ F. Wolfgramm, Y. A. de Icaza Astiz, F. A. Beduini, A. Cerè, and M. W. Mitchell, *Phys. Rev. Lett.* **106**, 053602 (2011).
 - ³¹ A. Ahlrichs and O. Benson, *Applied Physics Letters* **108**, 021111 (2016).
 - ³² M. Förtsch, G. Schunk, J. U. Fürst, D. Strekalov, T. Gerrits, M. J. Stevens, F. Sedlmeir, H. G. L. Schwefel, S. W. Nam, G. Leuchs, and C. Marquardt, *Phys. Rev. A* **91**, 023812 (2015).
 - ³³ K.-H. Luo, H. Herrmann, S. Krapick, B. Brecht, R. Ricken, V. Quiring, H. Suche, W. Sohler, and C. Silberhorn, *New Journal of Physics* **17**, 073039 (2015).
 - ³⁴ D. Rielander, J. Fekete, M. Cristiani, and H. de Riedmatten, in *Lasers and Electro-Optics Europe (CLEO EUROPE/IQEC), 2013 Conference on and International Quantum Electronics Conference* (IEEE, 2013) pp. 1–1.
 - ³⁵ M. Ebrahim-Zadeh, *Handbook of Optics* **4** (2010).
 - ³⁶ R. C. Eckardt, C. Nabors, W. J. Kozlovsky, and R. L. Byer, *JOSA B* **8**, 646 (1991).
 - ³⁷ A. Henderson, M. Padgett, F. Colville, J. Zhang, and M. Dunn, *Optics communications* **119**, 256 (1995).
 - ³⁸ C. Nabors, S. Yang, T. Day, and R. Byer, *JOSA B* **7**, 815 (1990).
 - ³⁹ F. Wolfgramm, *Atomic quantum metrology with narrow-band entangled and squeezed states of light*, Ph.D. thesis, Universitat Politècnica de Catalunya (2012).
 - ⁴⁰ U. Schünemann, H. Engler, R. Grimm, M. Weidemüller, and M. Zielonkowski, *Review of Scientific Instruments* **70**, 242 (1999).
 - ⁴¹ M. Scholz, L. Koch, and O. Benson, *Physical review letters* **102**, 063603 (2009).
 - ⁴² C. Clausen, F. Bussièeres, A. Tiranov, H. Herrmann, C. Silberhorn, W. Sohler, M. Afzelius, and N. Gisin, *New Journal of Physics* **16**, 093058 (2014).
 - ⁴³ M. Scholz, L. Koch, and O. Benson, *Optics Communications* **282**, 3518 (2009).
 - ⁴⁴ R. Y. Rubinstein and D. P. Kroese, *Simulation and the Monte Carlo Method (Wiley Series in Probability and Statistics)*, 2nd ed.
 - ⁴⁵ P.-J. Tsai and Y.-C. Chen, *Quantum Science and Technology* **3**, 034005 (2018).
 - ⁴⁶ K. Niizeki, K. Ikeda, M. Zheng, X. Xie, K. Okamura, N. Takei, N. Namekata, S. Inoue, H. Kosaka, and T. Horikiri, *Applied Physics Express* **11**, 042801 (2018).
 - ⁴⁷ V. Tamma and S. Laibacher, *Physical review letters* **114**, 243601 (2015).
 - ⁴⁸ J. Yang, X.-H. Bao, H. Zhang, S. Chen, C.-Z. Peng, Z.-B. Chen, and J.-W. Pan, *Physical Review A* **80**, 042321 (2009).